

AN INSIGHT INTO PINEAPPLE PEEL WASTE ADSORBENT FOR IRON CONTAMINATED WATER THROUGH KINETIC AND ISOTHERM STUDY

(Tinjauan Terhadap Penjerap daripada Sisa Kulit Nanas bagi Air Tercemar dengan Ferum Melalui Kajian Kinetik dan Isotherma)

Nurul Faizah Abd Ghapar¹, Rozaimi Abu Samah^{1*}, Mohamad Syafiq Abdul Wahab², Sunarti Abd Rahman¹, and Mohd Hafiz Dzarfan Othman³

¹Faculty of Chemical & Process Engineering Technology, Universiti Malaysia Pahang Al-Sultan Abdullah, Lebuhr Persiaran Tun Khalil Yaakob, 26300 Kuantan, Pahang, Malaysia.

²EMZI-UiTM Nanoparticles Colloids and Interface Industrial Research Laboratory (NANO-CORE), School of Chemical Engineering, College of Engineering, Universiti Teknologi MARA, Cawangan Pulau Pinang, Kampus Permatang Pauh, 13500 Permatang Pauh, Penang, Malaysia.

³Advanced Membrane Technology Research Center (AMTEC), School of Chemical and Energy Engineering, Universiti Teknologi Malaysia, 81310 UTM Johor Bahru, Johor, Malaysia

*Corresponding author: rozaimi@ump.edu.my

Received: 17 November 2023; Accepted: 12 February 2024; Published: 29 April 2024

Abstract

The swift growth of sectors like steel and coal mining leads to a higher release of heavy metals like iron into aquatic ecosystems, resulting in water pollution. In this study, the kinetics and isotherms studies were applied to pineapple peel waste based adsorbent for iron removal. An adsorbent derived from discarded pineapple peels was created through a chemical activation process, employing zinc chloride ($ZnCl_2$) as the activator. By examining the effects of various experimental parameters, including contact duration (30–240 min), concentration of iron (5–80 ppm), and the amount of adsorbent (2–24 g/L), the behaviour of the adsorbent for iron adsorption was carefully studied. Maximum iron removal of 99.24% efficiency with adsorbent dosage of 20 g/L was achieved through this study. The iron removal process was most accurately represented by the Freundlich isotherm model, exhibiting an R^2 value of 0.985. Furthermore, the kinetics investigation demonstrated an excellent fit with the pseudo-second-order model for iron adsorption, yielding an R^2 value of 0.999. These findings strongly indicate that pineapple peel waste holds promise as a viable adsorbent for eliminating iron from water bodies.

Keywords: Pineapple peel waste, iron removal, adsorption isotherm, adsorption kinetic

Abstrak

Pertumbuhan pesat sektor-sektor seperti keluli dan perlombongan arang menyebabkan peningkatan pelepasan logam berat seperti ferum ke dalam ekosistem akuatik, yang mengakibatkan pencemaran air. Dalam kajian ini, kajian kinetik dan isoterma telah digunakan bagi penyingkiran ferum menggunakan penjerap berasaskan sisa kulit nanas. Penjerap yang diperolehi daripada kulit nanas yang dibuang telah dihasilkan melalui proses pengaktifan kimia dengan menggunakan zink klorida ($ZnCl_2$) sebagai pengaktif. Dengan mengkaji kesan pelbagai parameter eksperimen, termasuk tempoh penjerapan (30–240 minit), kepekatan ferum (5–80 ppm), dan jumlah penjerap (2–24 g/L), tingkah laku penjerap untuk penjerapan ferum telah dikaji dengan teliti. Penyingkiran ferum maksimum sebanyak 99.24% dengan dos penjerap 20 g/L telah dicapai melalui kajian ini. Proses penyingkiran ferum paling tepat

diwakili oleh model isoterma Freundlich, dengan nilai R^2 sebanyak 0.985. Selain itu, penyiataan kinetik menunjukkan kesesuaian yang sangat baik dengan model pseudo-tertib kedua untuk penjerapan ferum, menghasilkan nilai R^2 sebanyak 0.999. Penemuan ini menunjukkan bahawa sisa kulit nanas berpotensi sebagai penjerap yang berkesan untuk menyinkirkan ferum dari air.

Kata kunci: sisa kulit nenas, penyingkiran ferum, isoterma penjerapan, kinetik penjerapan

Introduction

Iron stands as one of the most plentiful elements in the earth's crust, occurring naturally in water in two primary forms: soluble ferrous iron, Fe(II) or $\text{Fe}(\text{OH})^+$, and complexed ferric iron, Fe(III), which precipitates as $\text{Fe}(\text{OH})_3$ [1]. Iron can also be found in water because of industrial activities like metal plating, mining, the iron and steel industry, and the corrosion of metal materials [1, 2]. As reported by Al-Anber, the safe level for Fe(III) ions for the human body is not more than 0.3 ppm and excessive iron ions may cause anorexia and oliguria. The high amount of iron can also give the water a metallic taste and odour [3]. To overcome these problems, special attention should be given to removing or reducing the amount of iron ions from industrial water effluents or water supply.

Liquid-phase adsorption is one of the most common methods used to remove heavy metals from wastewater due to the proper design of the adsorption process that will produce a high-quality treated effluent [2]. However, the adsorption of heavy metals such as iron by commercial adsorbent is expensive; therefore, research studies focus on developing adsorbents from agricultural waste to remove iron from the aqueous system [3]. Among these various adsorbents, including rice hull [2], rice husk ash [4], orange peel [5], olive stones [1, 6], wild jack, and jambul barks [7] have been employed for the purpose of eliminating iron ions from aqueous solutions. Based on recent works, adsorbent from pineapple peel waste can be considered an agricultural waste that shows remarkable potential towards the adsorption of toxic heavy metals from the aqueous solutions. For instance, Zn, Cr, Cd, Pb, Mn, and Cu ions have been removed from aqueous solutions [8–11].

Malaysia's pineapple (*Ananas comosus*) industry was ranked 18th world's largest pineapple producer with 334,400 metric tonnes produced by 13,733 hectares of planted area. As reported by Ahmad Zamri et al., about 335,488 tonnes of pineapple produced in Malaysia yielded 137,550 tonnes of pineapple peel [12]. Pineapple fruit typically consists of around 60% edible flesh and

approximately 35% skin or peel, which is considered waste material. This peel is primarily composed of cellulose, hemicellulose, lignin, and pectin substances. With certain modifications, pineapple peel can be repurposed and utilised as an adsorbent material [10, 11]. Previous studies reported adsorbent from pineapple peel waste showed very high removal efficiencies of heavy metals such as Cd(II), Pb(II), Cu(II), Zn(II), and Cr(VI). For example, Turkmen et al. reported that the pineapple peel waste which was carbonised using microwave at 800 W yielded a maximum Zn(II) removal efficiency of 93% for both types of activating agent: ZnCl_2 and H_2SO_4 [13]. The similar result reported by Olowu et al. (2022) when pineapple peel adsorbent was used to remove Zn(II) and Cr(VI) from the aqueous solution with the maximum percentage removals of 89% and 91.2%, respectively [8]. Hence, considering both economic and environmental aspects, pineapple peel waste may serve as an effective adsorbent for the removal of iron from aqueous solutions.

Solid waste derived from processed pineapple peel waste has previously been employed as an adsorbent, demonstrating considerable potential for adsorbing harmful pollutants, including heavy metals. In this study, we assessed the capability of pineapple peel waste as an adsorbent for capturing Fe(III) ions from aqueous solutions. The investigation involved the assessment of various operational factors such as contact time, adsorbent quantity, and initial iron concentration through a batch adsorption study. Furthermore, we delved into the sorption mechanism by examining different kinetic models, including the pseudo-first- and pseudo-second-order models. To evaluate various isotherms and their capacity to correlate with experimental data, three isotherm models—Langmuir, Freundlich, and Temkin—were employed.

Materials and Methods

Materials

Iron standard solution, $\text{Fe}(\text{NO}_3)_3$, sulfuric acid, H_2SO_4 , and zinc chloride, ZnCl_2 , of analytical grade were procured from Merck chemicals. A stock iron solution

with a concentration of 1,000 mg/L was employed as the adsorbate, and different concentrations were prepared by diluting the stock solution with distilled water. pH measurements were conducted using the pH meter pH 150 from Eutech Instruments.

Preparation of adsorbent from pineapple peel waste

The adsorbent was prepared using a method reported by Rozaidi & Abu Samah with some modifications [14]. Pineapple peel waste collected from Pekan Pina Sdn. Bhd. was washed with distilled water. The peels were oven-dried at 80 °C for 24 h. Then, the dried peels were ground and sieved using a sieve with 300 µm size to obtain the particle size of less than 300 µm. After that, chemical activation was performed by mixing 30 g of sieved pineapple peels with 1.0 M of ZnCl₂. The procedure involved stirring the mixture for 24 h at room temperature using a magnetic stirrer, followed by filtration. The filtered peels were then dried in an oven at 80 °C overnight. Subsequently, the sample was placed in a sealed crucible and subjected to carbonisation at 800 °C for 1 h, with a heating rate of 10 °C per min. After cooling to room temperature, the sample was immersed in a 0.5 M H₂SO₄ solution for 30 min to remove the excess ZnCl₂. Following this, the sample was once again dried in an oven at 80 °C for 24 h after being filtered and washed with distilled water until the wash water reached a pH of 7. The samples were then transferred to a desiccator and stored in sealed plastic bags for future use [15].

Characterisation of adsorbent

To identify the primary functional groups, present in the adsorbent, Fourier transform infrared spectroscopy (FTIR) was employed, utilising a Nicolet AVATAR 370 DTGS, UK instrument. The analysis covered the functional groups within the samples across a range of 500–4500 cm⁻¹. FTIR analysis allows the samples to be absorbed at different wavelengths with characteristic beams produced at different wavelengths which will later be analysed and computerised in the form of wave numbers, expressed in cm⁻¹. All spectra included the wave numbers from 4000 to 500 cm⁻¹ with 128 scans at a resolution of 2.0 cm⁻¹.

Furthermore, the adsorbents were pretreated by degassing at 200 °C for 2 h, in a vacuum condition, then the specific Brunauer–Emmett–Teller analysis (BET,

Micromeritics ASAP 2010, USA) was used to determine the surface area (S_{BET}) of the samples.

Additionally, the morphology of the adsorbent was examined through scanning electron microscopy (SEM, JEOL JSM-7800F, Japan). The adsorbent was mounted using a carbon conductive pad on a metal stub and silver metals were placed at both sides of the samples. In a vacuum condition of an argon atmosphere, the samples were coated with gold for observation and analysis. When the scanning completed, the results were shown based on image formed at SEM display unit.

Batch adsorption study

Batch adsorption experiments were performed under standard conditions, where 2 g/L of the pineapple peel waste adsorbent was mixed with an iron-containing aqueous solution. The stirring process took place at ambient temperature and pressure. The mixture was continuously stirred magnetically for a duration of 240 min. To monitor the adsorption process over time, 10 mL of the mixture were withdrawn at 30-min intervals, and the amount of iron in these samples was analysed. The iron content was determined by using an atomic absorption spectrometer (AAS AAnalyst 400, Perkin Elmer). The experiment was repeated with different amounts of adsorbent (2–24 g/L) and different initial concentrations of iron (5–30 ppm). The removal of iron by the adsorbent was calculated using Equation 1.

$$\text{Removal (\%)} = \frac{C_i - C_t}{C_i} \times 100 \% \quad (1)$$

C_i represents the initial iron concentration in the sample (measured in mg/L), while C_t denotes the concentration of iron at a particular time during the experiment (also measured in mg/L).

The amount of iron adsorbed on the adsorbent at certain time was calculated using Equation 2:

$$q_t = \frac{(C_i - C_t)V}{M} \quad (2)$$

Here, q_t represents the iron adsorption on the adsorbent at any given time (measured in mg/g), V indicates the volume of the solution in litres (L), and M signifies the mass of the adsorbent in grams (g).

Kinetic modeling

Pseudo-first- and pseudo-second-order kinetic models are commonly used to describe the adsorption kinetics [16]. The pseudo-first-order equation is given by Equation 3:

$$\frac{dq_t}{dt} = k_1 (q_e - q_t) \quad (3)$$

where q_t and q_e are the amount of solute adsorbed (mg/g) at time t and equilibrium, respectively and k_1 is the rate constant of the kinetic model (min^{-1}). The linearised equation of pseudo-first-order can be expressed by Equation 4:

$$\log(q_e - q_t) = \log q_e - \frac{k_1}{2.303} t \quad (4)$$

A plot of $\log(q_e - q_t)$ versus t can be used to obtain the rate constant.

The pseudo-second-order equation is expressed by Equation 5:

$$\frac{dq_t}{dt} = k_2 (q_e - q_t)^2 \quad (5)$$

where k_2 is the pseudo-second-order rate constant ($\text{g/mg}\cdot\text{min}$) and the linearised form is expressed in Equation 6:

$$\frac{t}{q_t} = \frac{1}{k_2 q_e^2} + \frac{1}{q_e} t \quad (6)$$

A plot of t/q_t versus t gives the pseudo-second-order rate constant.

Adsorption Isotherms

Langmuir, Freundlich, and Temkin isotherms are commonly used to determine the adsorption isotherms. These equations explain the relationship between the solute concentrations in both liquid and adsorbent surface equilibrium. Equation 7 represents the Langmuir isotherms:

$$q_e = \frac{q_m K_L C_e}{1 + K_L C_e} \quad (7)$$

where q_e is the quantity of the adsorbed adsorbate bound per unit amount of adsorbent (mg/g), q_m is the maximum adsorption capacity, K_L is the affinity constant for Langmuir isotherm (L/mg), and C_e is the adsorbate equilibrium concentration (mg/L).

To determine the values of maximum adsorption capacity (q_m) and the Langmuir affinity constant (K_L), Equation 7 can be linearised into several form as shown in Equation 8.

$$\frac{C_e}{q_e} = \frac{C_e}{q_m} + \frac{1}{q_m K_L} \quad (8)$$

A plot of C_e/q_e versus C_e was plotted to determine the values of q_m and K_L .

Freundlich isotherm does not predict the saturation binding of the adsorption. It assumes a logarithmic relationship between the adsorption equilibrium and the solute concentration as shown in Equation 9.

$$q_e = K_F C_e^{1/n} \quad (9)$$

where K_F is known as the Freundlich constant (mg/g) and $1/n$ is a constant reflecting the solute affinity towards the adsorbent.

By taking logarithmic on both sides of the equation, a linearised form of Freundlich isotherm can be used as shown in Equation 10 to determine the adsorption constant (K_F) and its affinity ($1/n$) by plotting $\log q_e$ versus $\log C_e$.

$$\log q_e = \log K_F + \frac{1}{n} \log C_e \quad (10)$$

The Temkin isotherm model infers that the adsorption energy decreases linearly with the surface coverage caused by adsorbent–adsorbate interactions [3]. The Temkin isotherm is described in Equation 11:

$$q_e = B \ln A + B \ln C_e \quad (11)$$

where C_e is the adsorbate equilibrium concentration (mg/L) and q_e is the quantity of metal adsorbed per gram of the adsorbent (mg/g).

The Temkin isotherm equation can be linearised to Equation 12:

$$q_e = \frac{RT}{b} \ln C_e + \frac{RT}{b} \ln K_T \quad (12)$$

where $RT/b = B$ (J/mol) and $K_T = A$ (L/g) are the Temkin constants. R (8.314 J/mol·K) represents the universal gas constant at T (K) which is the absolute solution temperature.

A plot q_e versus $\ln C_e$ was plotted to determine the Temkin constant.

Results and Discussion

Characterisation of pineapple peel waste adsorbent: BET analysis

The Brunauer–Emmett–Teller (BET) surface area measurement was utilised to assess the adsorption capacity of the adsorbent. This measurement operates on the principle that a greater surface area of the adsorbent corresponds to a higher adsorption capacity. In other words, as the surface area of the adsorbent increases, its ability to adsorb substances, in this case, iron, also increases. This relationship underscores the importance of surface area in determining the effectiveness of the adsorbent in adsorbing the target substance [17]. After chemical treatment followed by carbonisation at 800 °C for 1 hour, the surface area of pineapple peel waste adsorbent obtained was 1080.91 m²/g. A prior study documented that following the activation and carbonisation procedures applied to raw pineapple peel waste, there was a noteworthy enhancement in the surface area of the prepared adsorbent [18]. Besides, the surface area of raw pineapple peel waste was 7.9348

m²/g [14]. The carbonisation process conducted at 800 °C had the effect of improving the elimination of volatile compounds. Additionally, the inclusion of ZnCl₂ as an impregnation agent heightened the heat energy within the process. This, in turn, led to the creation of new pores and an accelerated development of porosity in the adsorbent. Consequently, these factors collectively contributed to an increase in the surface area of the adsorbent. [19].

The N₂ adsorption isotherms for the adsorbent are depicted in Figure 1. The behaviour of the adsorbent corresponds to a Type I isotherm, indicating that the adsorbent possesses microporous characteristics. A Type I isotherm typically exhibits a convex curve, and its plateau is either horizontal or nearly horizontal. In this type of isotherm, the adsorption curve directly intersects with the line $P/P_0 = 1$ [18]. The amount of adsorption experienced a rapid increase in a region of low relative pressure ($P/P_0 < 0.2$) during the initial stages of adsorption. This observation suggests that the primary location for nitrogen molecule adsorption was within the microporous structure of the adsorbent [18].

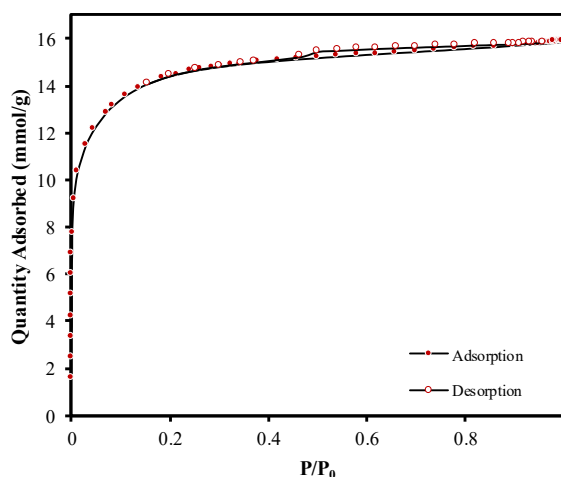


Figure 1. N₂ adsorption–desorption isotherms of adsorbent

Scanning electron microscopy (SEM) of adsorbent

Figure 2 shows the SEM images of raw pineapple peel waste, the prepared pineapple peel waste adsorbent, and the adsorbent after the adsorption process. SEM analysis was employed to observe the surface morphologies of the raw pineapple peel waste, the prepared adsorbent at 800 °C for 1 h, and the adsorbent after adsorption. The

surface of raw pineapple peel waste is naturally uneven and features creases. However, the surface of the adsorbent exhibits a more intricate and porous structure after the modification process. This transformation can be attributed to the removal of volatile substances during carbonisation and activation, resulting in a stable carbon mass and the widening of pore networks within the

adsorbent sample, as documented in reference [20]. The porous nature of the adsorbent plays a significant role in facilitating the adsorption of heavy metals in wastewater. These pores serve as active sites for adsorption and increase the overall surface area of the adsorbent, as discussed in reference [21]. Furthermore, in this study, it was noted that the adsorbent's surface featured densely packed bundles of elongated cylindrical pores, signifying a strong adsorption

capacity. This configuration provides an abundance of sites for capturing heavy metal ions, such as iron. This could be explained by the morphology of the adsorbent after adsorption where the surface morphology became rougher or more irregular due to the formation of metal ion complexes or precipitates on the surface of the adsorbent. It was observed that there are some cavities on the surface of the adsorbents [22].

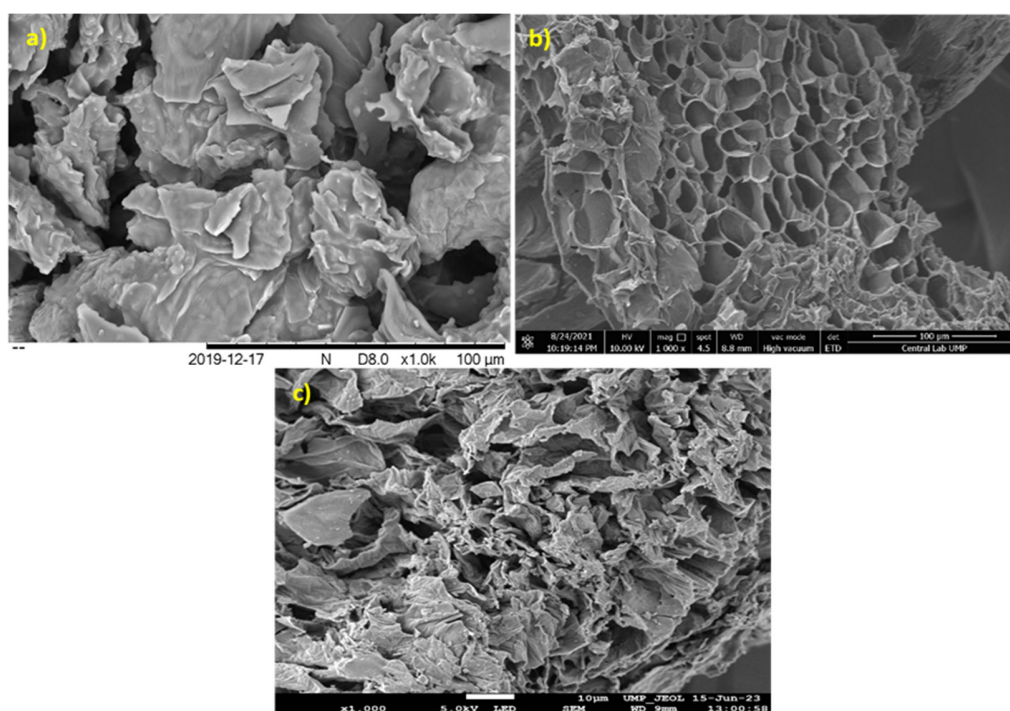


Figure 2. SEM images (1000× magnification) of (a) raw pineapple peel waste, (b) pineapple peel waste adsorbent and (c) adsorbent after adsorption

FTIR analysis

FTIR analysis was conducted to qualitatively identify the primary functional groups present on the surface of the adsorbent derived from pineapple fruit peel. Figure 3 displays the FTIR spectra of both the adsorbent and the raw pineapple peel. In the spectrum of the raw pineapple peel, a broad band appearing around $3,300\text{ cm}^{-1}$ is primarily associated with hydrogen bonds (O–H or NH_2) symmetrical stretching variations. Additionally, the peak at $2,917\text{ cm}^{-1}$ corresponds to aliphatic CH groups.

However, after the modification process, several peaks within the range of $1,560\text{--}1,300\text{ cm}^{-1}$ can be attributed to CH_2 bending vibrations, O–H bending, and O–H stretching or C– bending vibrations. Furthermore, a strong band at $1,089\text{ cm}^{-1}$ is attributed to the C–O of the $-\text{OCH}_3$ group, aligning with the lignin structure present in pineapple fruit peel [10] and [21]. The slight shift in absorption bands indicates the successful transformation of the raw pineapple peel into the adsorbent.

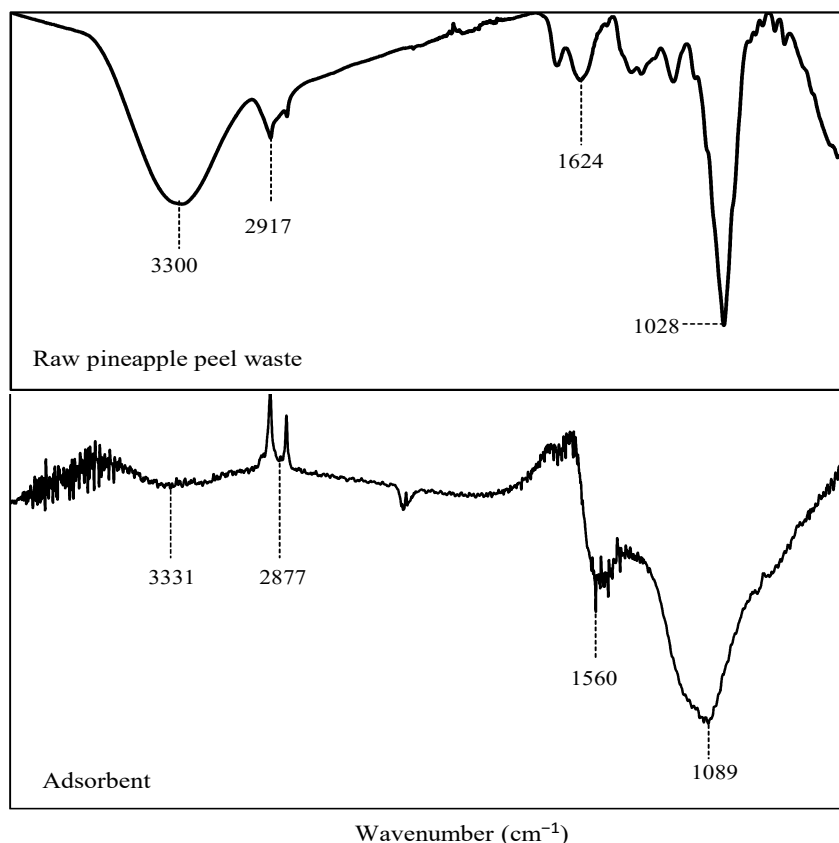


Figure 3. FTIR spectra for the raw pineapple peel waste and pineapple peel waste adsorbent

Batch adsorption studies: The effect of contact time

One of the most critical factors affecting adsorption performance is the contact time, as it illustrates the removal percentage of metal ions from the solution over time [24]. The effect of contact time on iron adsorption onto the pineapple peel waste adsorbent is shown in Figure 4(a). In the initial stages, the rate of adsorption exhibited a substantial increase and gradually reached equilibrium around the 150-min mark, achieving an efficiency of approximately 48.86% removal. Then, the final Fe(III) ions concentration became almost similar until 240 min. Therefore, the process was at steady state at 150 min. This situation happened when the metal ions rapidly adsorbed onto the adsorbent at the beginning caused by the availability of the empty active sites. In addition, the uptakes were gradually slower due to the decrease in vacant active sites [10]. It was reported that the properties of the adsorbent and its existing active sites are known to affect the time needed to reach equilibrium [23, 24].

The effect of adsorbent dosage

The impact of adsorbent dosage on the adsorption of iron onto the pineapple peel waste adsorbent was explored, as adsorbent dosage is recognised as another key factor influencing the adsorbent's capacity to adsorb metal ions at a given initial concentration [25–27]. In Figure 4(b), the removal percentage of Fe(III) ions and the adsorption capacity of the pineapple peel waste adsorbent are depicted across various dosages, all while maintaining a constant initial concentration of 5 ppm Fe solution. The graph demonstrates that 20 g/L gave the highest iron removal up to 99.24% and remained constant till 24 g/L. A higher amount of adsorbent dosage will increase the number of active sites since the adsorption depends on the availability of binding sites for iron [30].

The effect of initial iron concentration

In batch adsorption processes, the adsorption rate is a function of the initial concentration of heavy metal ions; hence it is a principal factor for a successful adsorption

process [31]. The percentage removal of iron at different initial concentrations from 5 to 80 ppm is shown in Figure 4(c). The removal efficiency increased drastically at 5 ppm before increasing gradually until 80 ppm with the highest removal of 80.13%. It shows that the pineapple peel waste adsorbent had a higher magnitude for Fe(III) ions adsorption. This may also be related to

an increase in the concentration gradient driving force with the increase in metal ions concentration [4]. A comparable result was also reported where the adsorption of iron using rice husk ash gave higher iron adsorption capacity than manganese, which means that increasing the initial concentration of iron also improves the removal efficiency of iron [4].

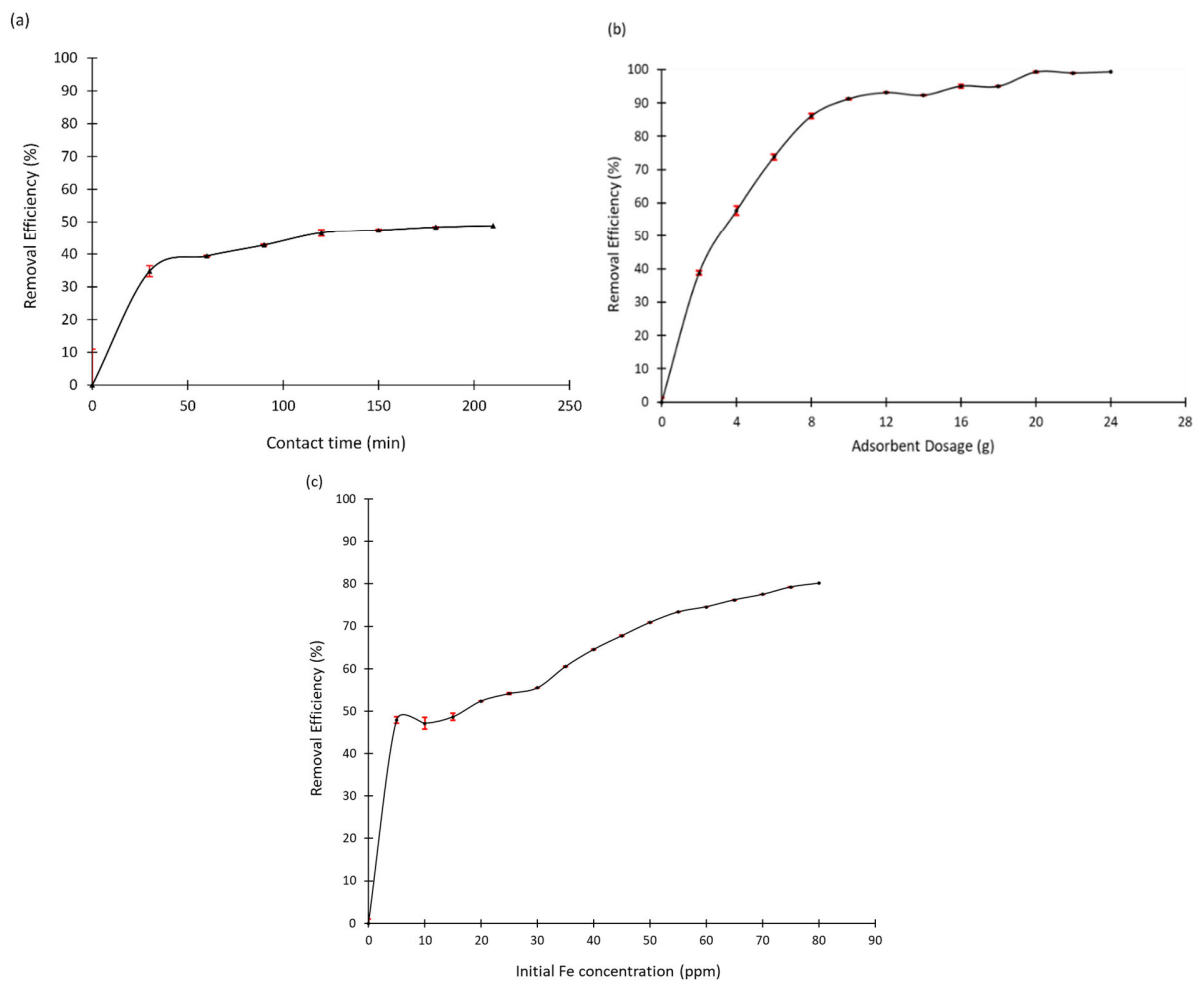


Figure 4. The effect of (a) contact time, (b) adsorbent dosage, and (c) initial iron concentration on the iron removal efficiency

Adsorption kinetic

Adsorption kinetics are used to explain the adsorption mechanism and characteristics. The pseudo-first- and pseudo-second-order kinetics models were applied to the adsorption data to specify the rate of adsorption of

iron onto the pineapple peel waste adsorbent. Constants of pseudo-first- and pseudo-second-order were determined from the slope and intercept of the linear plots as shown in Figure 5(a) and 5(b), respectively.

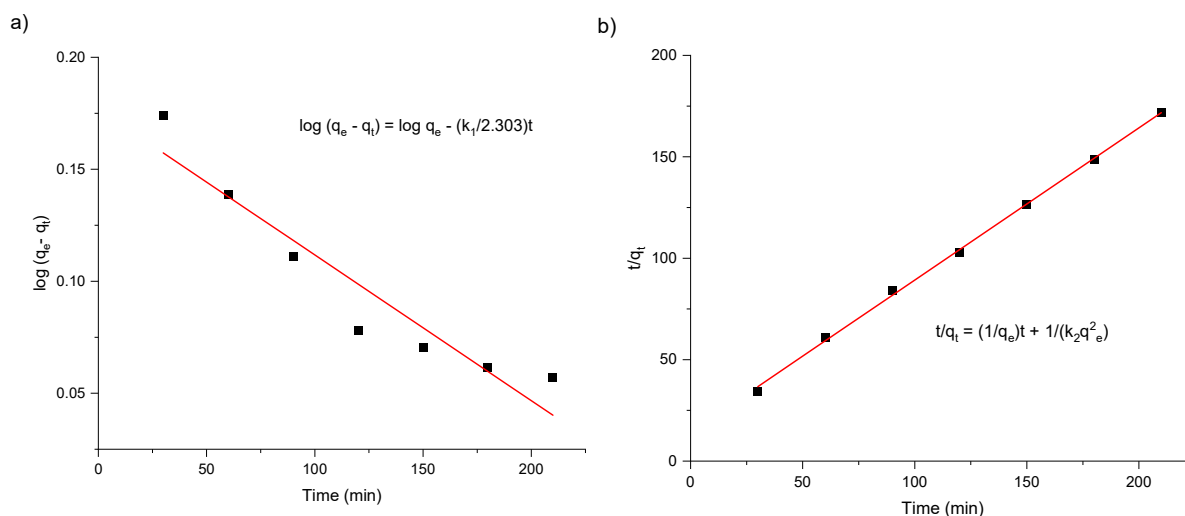


Figure 5. The plots of (a) pseudo-first- and (b) pseudo-second-order kinetic models for iron removal

Table 1. Pseudo-first- and pseudo-second-order parameters for iron removal

Model	Intercept	Slope	q _e (exp) (mg/g)	q _e (cal) (mg/g)	q ² _e	k	R ²
Pseudo-first-order	0.01535	-0.01228	1.198	-4.17664		0.028281	0.93689
Pseudo-second-order	14.19527	0.75037		1.332676	1.776025	0.039665	0.99872

Table 1 presents the parameters and regression coefficients (R^2) for both the pseudo-first-order and pseudo-second-order kinetic models. It is noteworthy that the pseudo-second-order model demonstrates a notably higher correlation coefficient ($R^2 > 0.9987$) in comparison to the pseudo-first-order model. This high R^2 value, close to unity, signifies a robust relationship between the parameters and underscores the suitability of the pseudo-second-order kinetic equation for describing the uptake of Fe(III) by the pineapple peel waste adsorbent [32]. Meanwhile, the equilibrium removal capacity calculated ($q_{e, cal}$) of the pseudo-second-order model was much closer to the equilibrium removal capacity experimental ($q_{e, exp}$) representing that the pseudo-second-order rate model gives a better summary of iron removal from solution to the pineapple

peel waste adsorbent. This conveys that the pseudo-second-order model can assume a chemically rate-controlling removal process [33].

The comparison of kinetics results with values from other studies is listed in Table 2. Iron adsorption onto the pineapple peel waste adsorbent was inferred to follow pseudo-second-order kinetics. These findings suggest that the rate-limiting step in the adsorption process is chemisorption, which entails valency forces, including the sharing or exchange of electrons between the adsorbent and the adsorbate [31, 34]. These results are consistent with previous literature, which also indicated that the adsorption kinetics of Fe(III) ions by distinct types of adsorbents typically adhere to the pseudo-second-order model [4, 32].

Table 2. Kinetic parameters comparison of iron adsorption onto various adsorbents

Adsorbent	Pseudo-first-order model		Pseudo-second-order model			References
	k ₁ (min ⁻¹)	R ²	k ₂ (g/mg·min)	q _e	R ²	
Pineapple peel	0.0283	0.9369	0.0397	1.33	0.9987	This study
Natural Clay	0.056	0.986	0.02	7.42	0.998	[35]
Acid-activated clay	0.058	0.991	0.007	11.41	0.994	[35]
Natural zeolite	4.9	0.8558	0.22	8.70	0.9985	[36]
Orange peel	0.001	0.032	0.068	13.44	0.996	[5]

Adsorbent	Pseudo-first-order model		Pseudo-second-order model			References
	k_1 (min^{-1})	R^2	k_2 ($\text{g}/\text{mg}\cdot\text{min}$)	q_e	R^2	
Limestone	0.069	0.919	5.913	0.019	0.997	[37]
Rice hull	0.017	0.90	0.000813	22.73	0.99	[2]
Natural feldspar	0.0283	0.83	0.0352	8.72	0.9987	[3]
Rice husk ash	-	-	0.033	1.340	0.995	[4]

Adsorption isotherms

An isotherm characterises the equilibrium association between the solute molecules bound to the adsorbent's surface and those remaining unbound in the liquid phase. In this study, Langmuir, Freundlich, and Temkin isotherms were employed to elucidate the equilibrium

relationship between the concentration of solute in the liquid phase and its interaction with the adsorbent's surface. Batch adsorption isotherm experiments were conducted to investigate iron adsorption using the pineapple peel waste adsorbent at room temperature. The results of these adsorption isotherms are visually presented in Figure 6(a-c).

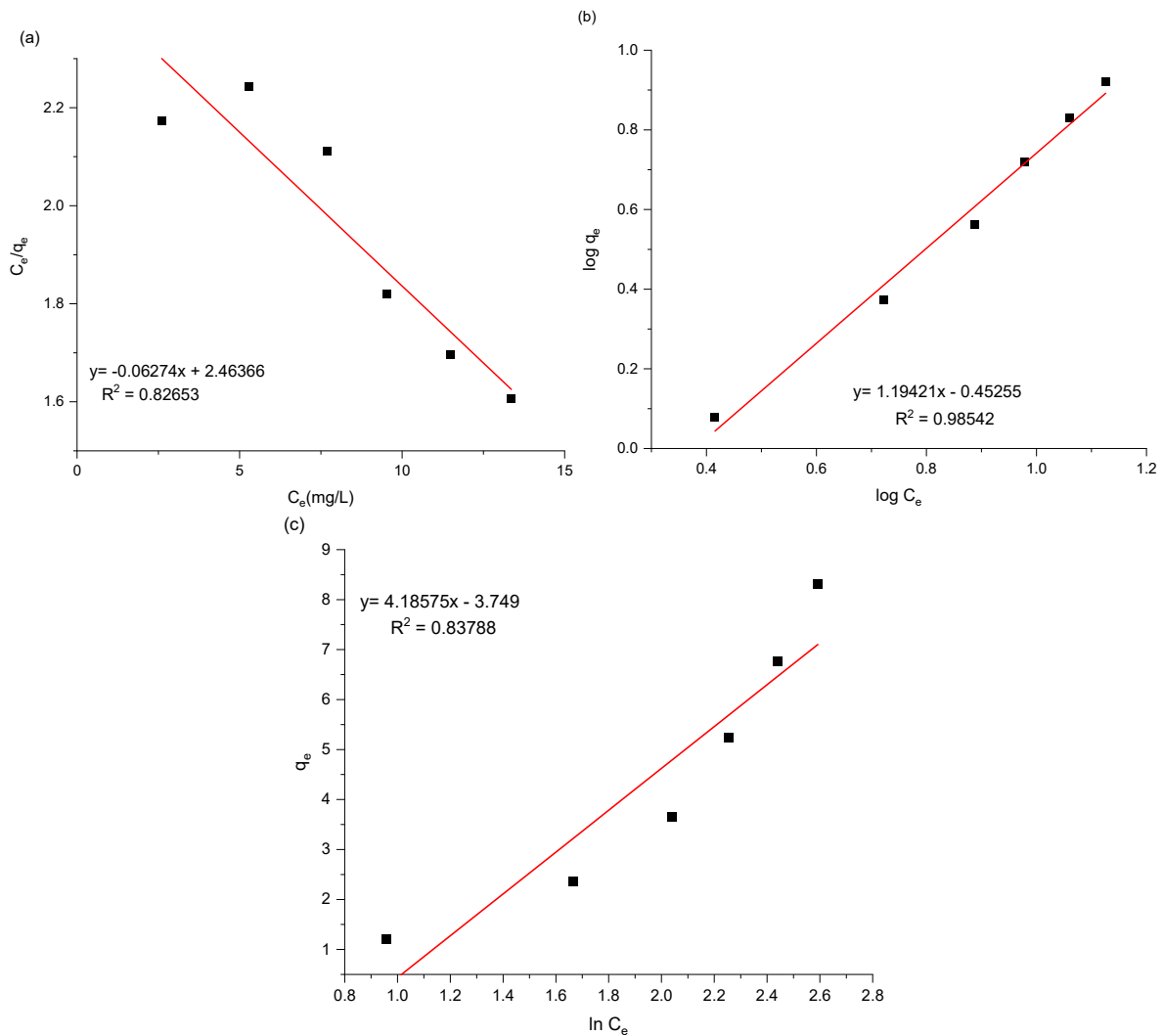


Figure 6. The plots of (a) Langmuir, (b) Freundlich, and (c) Temkin isotherms

Table 3. Langmuir, Freundlich, and Temkin isotherms parameters for iron removal

Isotherms	Constants	Value
Langmuir	$1/q_m$	0.0624
	q_m (mg/g)	15.9288
	K_L (L/mg)	0.0255
	R_L	1.1459
	R^2	0.8265
Freundlich	$1/n$	1.1942
	n	0.83737
	$\log K_F$	0.4526
	K_F (L/mg)	2.8349
	R^2	0.9854
Temkin	Slope = RT/B	4.1858
	Intercept = $RT/B (\ln A)$	-3.749
	B	597.8651
	A (L/mol)	0.3274
	R^2	0.8379

The results for all the parameters obtained from the Langmuir, Freundlich, and Temkin isotherms are summarised in Table 3. The Langmuir isotherm model was employed to fit the experimental data, yielding a correlation regression coefficient (R^2) of 0.8265. The maximum sorption capacity (q_m) was determined to be 15.94 mg/g using this model. However, it is evident that the data does not align well with the Langmuir model. This deviation may be attributed to interactions between the adsorbate or the fact that the adsorption process is not monolayer adsorption involving just one adsorbate molecule per adsorption site [38]. In this case, iron can be said to be adsorbed in inhomogeneous distribution to the adsorbent surface due to the irregular surface. So, there might be a ‘favoured’ point of strong adsorption

side. The results indicate that the Freundlich isotherm best fitted the iron adsorption on pineapple peel waste adsorbent with R^2 of 0.9854. However, with $1/n > 1$, it is best described by the S-type isotherm. This experiment agrees with the hypothesis that at low concentrations, such compounds compete with water for the adsorption sites. It means that the surface has a low affinity for the adsorbate at low concentrations, which then increases at higher concentrations [39]. On the other hand, the Temkin isotherm model moderately fitted the experimental data for iron adsorption onto pineapple peel waste adsorbent as the R^2 value is 0.84. The comparison of the adsorption capacity of other adsorbents for iron removal from aqueous solutions is tabulated in Table 4.

Table 4. Comparison of adsorption isotherms for iron removal using other adsorbents

Adsorbents	Langmuir			Freundlich			Temkin			References
	q (mg/g)	K_L (L/mg)	R^2	K_f (L/mg)	$1/n$	R^2	A	B	R^2	
Pineapple peel	15.93	0.0255	0.827	2.835	1.194	0.985	0.327	597.87	0.838	This study
Natural Clay	18.86	0.044	0.990	0.805	0.543	0.985				[35]
Acid-activated clay	25.00	0.09	0.998	5.96	0.312	0.993	-	-	-	[35]

Adsorbents	Langmuir			Freundlich			Temkin			References
	q (mg/g)	K_L (L/mg)	R^2	K_f (L/mg)	1/n	R^2	A	B	R^2	
Natural zeolite	6.13	17.92	0.977	6.04	0.3497	0.945	-	-	-	[36]
Spent coffee grounds	0.615	2.803	0.999	0.530	0.6606	0.991	-	-	-	[28]
Chitosan	133.3	0.0643	0.93	3.807	0.388	0.979	-	-	-	[40]
Limestone	0.018	140.31	0.923	0.029	0.216	0.753	-	-	-	[37]
Rice hull	45.45	0.03	0.99	1.07	0.68	0.97	32.27	28.36	0.79	[2]
Natural feldspar	25.00	0.046	0.936	1.701	0.622	0.997	-	-	-	[3]
Orange peel	8.35	0.15	0.998	4.97	0.0937	0.900	-	-	-	[5]
Rice husk ash	66.66	0.026	0.927	1.0739	0.916	0.908	54.5	101.76	0.93	[4]
Palm oil mill effluent	1.116	0.25	0.998	0.376	0.281	0.966	-	-	-	[41]

Proposed mechanisms of iron adsorption

Adsorbent from pineapple peel waste consists of three main components: cellulose, hemicellulose, and lignin. These cellulosic components contain a majority of the oxygen functional groups, such as hydroxyl, ether, and carbonyl, that influence the adsorption properties of the

iron onto the adsorbent [42]. The adsorbent after adsorption was examined using SEM analysis in Figure 2 and showed that the morphology of the adsorbent changed with the presence of some precipitation. The binding mechanism of the adsorbent and iron ions is proposed in Figure 7.

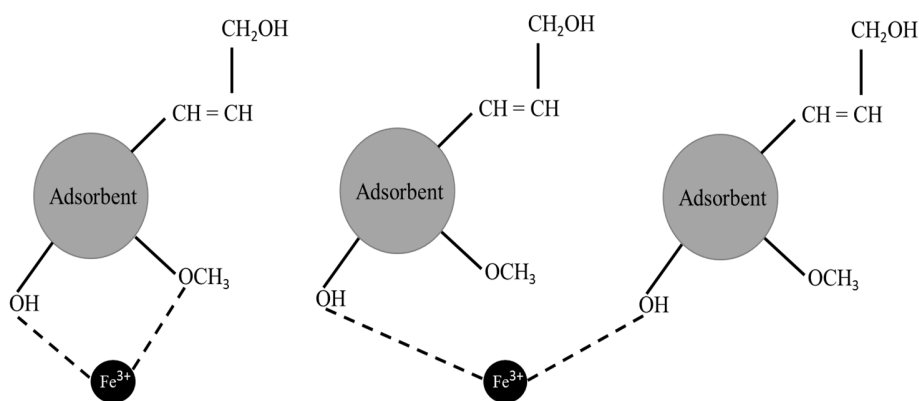


Figure 7. Binding mechanism of adsorbent and Fe(III) ions

Conclusion

In this study, the adsorbent from pineapple peel waste can potentially remove iron from wastewater. The results show that the adsorbent could remove 48.86% iron when 2 g/L of the adsorbent was used and increased to 99.24% when 20 g/L of the adsorbent was used. The adsorption isotherm study shows that iron adsorption fitted the experimental data of the Freundlich isotherm

rather than Langmuir and Temkin isotherms due to the highest R^2 value of 0.985. From the Langmuir model, the maximum iron adsorption capacity of the adsorbent was 15.93 mg/g. The adsorption kinetics study shows that iron adsorption followed the pseudo-second-order kinetics model, indicating that chemisorption was the mechanism of adsorption that contributed to the iron removal from the aqueous solution. Based on the results

of this study, pineapple peel waste adsorbent was found to be effective in removing iron from an aqueous solution.

Acknowledgements

The Ministry of Education Malaysia funded this study through the Fundamental Research Grant Scheme (FRGS) (RDU190126;FRGS/1/2018/TK02/UMP/02/8). Appreciations to Pekan Pina Sdn. Bhd. for providing the pineapple peel. We are grateful for the assistance from all the laboratory staff of the Faculty of Chemical & Process Engineering Technology, UMP.

References

1. Hodaifa, G., Ochando-Pulido, J. M., Ben Driss Alami, S., Rodriguez-Vives, S. and Martinez-Ferez, A. (2013). Kinetic and thermodynamic parameters of iron adsorption onto olive stones. *Industrial Crops Product*, 49: 526-534.
2. Abdel-ghani, N. T., El-chaghaby, G. A. and Zahran, E. M. (2015). Cost effective adsorption of aluminium and iron from synthetic and real wastewater by rice hull activated carbon (RHAC). *American Journal of Analytical Chemistry*, 6: 71-83.
3. Al-Anber, M. A. (2015). Adsorption of ferric ions onto natural feldspar: kinetic modeling and adsorption isotherm. *International Journal of Environmental Science and Technology*, 12(1): 139-150.
4. Adekola, F. A., Hodonou, D. S. S. and Adegoke, H. I. (2014). Thermodynamic and kinetic studies of biosorption of iron and manganese from aqueous medium using rice husk ash. *Journal of Applied Water Science*, 6: 319-330.
5. Surovka, D. and Pertile, E. (2015). Sorption of iron, manganese, and copper from aqueous solution using orange peel: Optimization, isothermic, kinetic, and thermodynamic studies. *Polish Journal of Environmental Study*, 26(2): 795-800.
6. Akl, M. A., Yousef, A. M. and AbdElnasser, S. (2013). Removal of iron and manganese in water samples using activated carbon derived from local agro-residues. *Journal of Chemical Engineering Process Technology*, 4(4):1-10.
7. Rose, E. P. and Rajam, S. (2012). Equilibrium study of the adsorption of iron (II) ions from aqueous solution on carbons from wild jack and jambul. *Advances in Applied Science Research*, 3(2): 1889-1894.
8. Olowu, R. A., Osundiya, M. O., Oyewole, T. S., Onwordi, C. T., Yusuff, O. K., Osifeko, O. L. and Tovide, O. O. (2022). Equilibrium and kinetic studies for the removal of Zn(II) and Cr(VI) ions from aqueous solution using pineapple peels as an adsorbent. *European Journal of Applied Sciences*, 10(5):34-47.
9. Mopoung, R. and Kengkhetkit, N. (2016). Lead and cadmium removal efficiency from aqueous solution by NaOH treated pineapple waste. *International Journal of Applied Chemistry*, 12(1): 23-35.
10. Ahmad, A., Khatoon, A., Mohd-Setapar, S. H., Kumar, R. and Rafatullah, M. (2016). Chemically oxidized pineapple fruit peel for the biosorption of heavy metals from aqueous solutions. *Desalination of Water Treatment*, 57(14): 6432-6442.
11. Hu, X., Zhao, M., Song, G. and Huang, H. (2011). Modification of pineapple peel fibre with succinic anhydride for Cu²⁺, Cd²⁺ and Pb²⁺ removal from aqueous solutions. *Environmental Technology*, 32(7): 739-746.
12. Ahmad Zamri, M. F. M., Akhlar, A., Mohd Roslan, M. E., Mohd Marzuki, M. H., Saad, J. M. and Shamsuddin, A. H. (2020). Valorisation of organic fraction municipal solid waste via anaerobic co-digestion of Malaysia tropical fruit for biogas production. *IOP Conference Series: Earth & Environmental Sciences*, 476(1):1-8.
13. Turkmen Koc, S. N., Kipcak, A. S., Moroydor Derun, E. and Tugrul, N. (2021). Removal of zinc from wastewater using orange, pineapple and pomegranate peels. *International Journal of Environmental Sciences & Technology*, 18(9): 2781-2792.
14. Rozaidi, N. I. M. and Abu Samah, R. (2018). Peel wastes of *Ananas comosus* (L.) Merr as biosorbent for Fe(II) Ions removal from aqueous solution. *Research Communication: Engineering Science & Technology Special issue Regional Chemical Engineering Undergraduate Congress (RCEUC)*, 1:8.
15. Abd Ghapar, N. F., Abu Samah, R. and Abd Rahman, S. (2020). Pineapple peel waste adsorbent for adsorption of Fe (III). *IOP Conferences Series: Materials & Science Engineering*, 991(012093): 1-5.

16. Liu, Y. and Shen, L. (2008). A general rate law equation for biosorption. *Biochemical Engineering Journal*, 38: 390-394.
17. Reddy, K. S. K., Al Shoaibi, A. and Srinivasakannan, C. (2015). Preparation of porous carbon from date palm seeds and process optimization. *International Journal of Environmental Sciences & Technology*, 12(3): 959-966.
18. Fu, B., Ge, C., Yue, L., Luo, J., Feng, D., Deng, H. and Yu, H. (2016). Characterization of biochar derived from pineapple peel waste and its application for sorption of oxytetracycline from aqueous solution. *BioResources*, 11(4): 9017-9035.
19. Saadia, M., Nazha, O., Abdlemjid, A. and Ahmed, B. (2012). Preparation and characterization of activated carbon from residues of oregano. *Journal of Surface Sciences & Technology*, 28(3): 91-100.
20. Das, D., Samal, D. P. and BC, M. (2015). Preparation of activated carbon from green coconut shell and its characterization. *Journal of Chemical Engineering Process Technology*, 6(5):1-12.
21. Ashtaputrey, S. D. and Ashtaputrey, P. D. (2016). Preparation, characterization and application of pineapple peel activated carbon as an adsorbent for water hardness removal. *Journal of Chemical and Pharmaceutical Research*, 8(8): 1030-1034.
22. Hossain, M. A., Kumita, M. and Mori, S. (2010). SEM characterization of the mass transfer of Cr(VI) during the adsorption on used black tea leaves. *African Journal of Pure Applied Chemistry*, 4(7): 135-141.
23. Mahamad, M. N., Ahmad Zaini, M. A. and Zakaria, Z. A. (2015). Preparation and characterization of activated carbon from pineapple waste biomass for dye removal. *International Biodeterioration & Biodegradation*, 102: 274-280.
24. Sazali, N., Harun, Z. and Sazali, N. (2020). A review on batch and column adsorption of various adsorbent towards the removal of heavy metal. *Journal of Advanced Research in Fluid Mechanics and Thermal Sciences*, 67(2): 66-88.
25. El-Sayed, G. O., Dessouki, H. A. and Ibrahim, S. S. (2011). Removal of Zn(II), Cd(II) and Mn(II) from aqueous solutions by adsorption on maize stalks. *Malaysian Journal of Analytical Sciences*, 15(1): 8-21.
26. Sekhararao Gulipalli, C., Prasad, B. and Wasewar, K. L. (2011). Batch study, equilibrium and kinetics of adsorption of selenium using rice husk ash (RHA). *Journal of Engineering Science & Technology*, 6(5): 590-609.
27. Desta, M. B. (2013). Batch sorption experiments: Langmuir and Freundlich isotherm studies for the adsorption of textile metal ions onto teff straw (eragrostis tef) agricultural waste. *Journal of Thermodynamic*, 1(1): 1-6.
28. Mohamed, K. N. and Yee, L. L. (2019). Removal of Fe Ion from polluted water by reusing spent coffee grounds. *Pertanika Journal of Science & Technology*, 27(3): 1077-1090.
29. Renu, Agarwal, M. and Singh, K. (2018). Removal of copper, cadmium, and chromium from wastewater by modified wheat bran using Box–Behnken design: Kinetics and isotherm. *Separation Science and Technology*, 53(10):1476-1489.
30. Nayeem, A., Mizi, F., Ali, M. F. and Shariffuddin, J. H. (2023). Utilization of cockle shell powder as an adsorbent to remove phosphorus-containing wastewater. *Environmental Research*, 216:1-8.
31. Kaur, R., Singh, J., Khare, R., Cameotra, S. S. and Ali, A. (2013). Batch sorption dynamics, kinetics and equilibrium studies of Cr(VI), Ni(II) and Cu(II) from aqueous phase using agricultural residues. *Applied Water Science*, 3(1): 207-218.
32. Seliem, M. K. and Komarneni, S. (2016). Equilibrium and kinetic studies for adsorption of iron from aqueous solution by synthetic Na-A zeolites: Statistical modeling and optimization. *Microporous Mesoporous Materials*, 228: 266-274.
33. Chen, J., Cai, Y., Clark, M. and Yu, Y. (2013). Equilibrium and kinetic studies of phosphate removal from solution onto a hydrothermally modified oyster shell material. *PLoS One*, 8(4):1-10.
34. Sahu, M. K., Mandal, S., Yadav, L. S., Dash, S. S. and Patel, R. K. (2016). Equilibrium and kinetic studies of Cd(II) ion adsorption from aqueous solution by activated red mud. *Desalination Water Treatment*, 57(30): 14251-14265.
35. Khalfa, L., Cervera, M. L., Souissi-Najjar, S. and Bagane, M. (2021). Removal of Fe(III) from synthetic wastewater into raw and modified clay: Experiments and models fitting. *Separation Science and Technology*, 56(4): 708-718.

36. Neag, E., Török, A. I., Tanaselia, C., Aschilean, I. and Senila, M. (2020). Kinetics and equilibrium studies for the removal of Mn and Fe from binary metal solution systems using a Romanian thermally activated natural zeolite. *Water (Switzerland)*, 12(6):1-13.
37. Akbar, N. A., Aziz, H. A. and Adlan, M. N. (2016). Potential of high quality limestone as adsorbent for iron and manganese removal in groundwater. *Jurnal Teknologi*, 78(9-4):77-82.
38. Doran, P. M. (2013). Bioprocess engineering principles. Chapter 11, John Wiley. pp: 445-595.
39. Younes, A. A., Abdulhady, Y. A. M., Shahat, N. S. and El-Din El-Dars, F. M. S. (2021). Removal of cadmium ions from wastewaters using corn cobs supporting nano-zero valent iron. *Separation Science and Technology*, 56(1):1-13.
40. Ali, M. E. A., Aboelfadl, M. M. S., Selim, A. M., Khalil, H. F. and Elkady, G. M. (2018). Chitosan nanoparticles extracted from shrimp shells, application for removal of Fe(II) and Mn(II) from aqueous phases. *Separation Science and Technology*, 53(18): 2870-2881.
41. Shavandi, M. A., Haddadian, Z., Ismail, M. H. S., Abdullah, N. and Abidin, Z. Z. (2012). Removal of Fe(III), Mn(II) and Zn(II) from palm oil mill effluent (POME) by natural zeolite. *Journal of the Taiwan Institute of Chemical Engineers*, 43(5): 750-759.
42. Al-Ghouti, M. A., Li, J., Salamh, Y., Al-Laqtah, N., Walker, G. and Ahmad, M. N. M. (2010). Adsorption mechanisms of removing heavy metals and dyes from aqueous solution using date pits solid adsorbent. *Journal of Hazardous Materials*, 176: 510-520.